Original Article

Composite glycidyl methacrylated dextran (Dex-GMA)/gelatin nanoparticles for localized protein delivery

Fa-ming CHEN[#,*], Zhi-wei MA[#], Guang-ying DONG, Zhi-fen WU

Department of Periodontology and Oral Medicine, School of Stomatology, Fourth Military Medical University, Xi'an 710032, China

Aim: Localized delivery of growth factors has significant potential as a future therapeutic strategy in tissue engineering and regenerative medicine. A nanoparticle vehicle was created and evaluated in this study with the intent to deliver growth factors for periodontal regeneration.

Methods: Novel composite nanoparticles based on glycidyl methacrylate derivatized dextrans (Dex-GMA) and gelatin were fabricated by a facile method without using any organic solvents. The configurations of the resultant nanoparticles were evaluated by transmission electron microscopy, scanning electron microscopy, and atomic force microscope. Their surfaces were characterized by zeta-potential measurements, after which their properties including swelling, degradation, drug release, and cytotoxicity were also investigated using *in vitro* models.

Results: The particle size of Dex-GMA/gelatin nanoparticles (DG-NPs) ranged from 20 to 100 nm and showed a mono-disperse size distribution (mean diameter 53.7 nm) and a strongly negative surface zeta potential (-20 mV). The DG-NPs were characterized by good swelling and degradation properties in media including dextranase. The *in vitro* drug release studies showed that the efficient bone morphogenetic protein (BMP) release from DG-NPs was maintained for more than 12 d under degradation conditions, where more than 90% of the loaded BMP was released. No any relevant cell damage caused by DG-NPs was found in the cytotoxicity tests for a period of 24 h.

Conclusion: These combined results demonstrate that DG-NPs fulfill the basic prerequisites for growth factor delivery. With further *in vivo* studies, those nanoparticles may offer a promising vehicle for the delivery of active drugs to the periodontium.

Keywords: drug delivery systems; drug carriers; bone morphogenetic protein; periodontal regeneration; growth factors

Acta Pharmacologica Sinica (2009) 30: 485–493; doi: 10.1038/aps.2009.15; published online 23rd March 2009

Introduction

The objective of regenerative medicine is to induce the repair of defective tissues based on the natural healing potential of patients. For successful tissue regeneration, it is indispensable to provide local cells with a natural cellular microenvironment by providing an artificial extracellular matrix (ECM) and by delivering growth factors; in such environment, cells can proliferate and differentiate efficiently[1]. The localized delivery of bioactive molecules is known to be key to this microenvironment, and a desired release technology often enhances the *in vivo* stability of growth factors and prolongs the maintenance of biological functions for tissue regeneration. Nonetheless, optimal methods of delivery remain to be identified[2, 3].

Among the possible strategies to achieve sufficient bioactivity and bioavailability of growth factors for tissue engineering and regeneration, nanoparticulate carriers synthesized from biodegradable polymers represent an exciting approach to increase the uptake and transport of locally administered therapeutic molecules[4, 5]. While biodegradable nano/microparticles of poly(*D*,*L*-lactide-co-glycolide) (PLGA) and PLGA-based polymers have been widely explored as carriers for the controlled delivery of macromolecular therapeutics (*eg*, proteins, peptides, vaccines, genes, antigens, and growth factors)[4], we are interested in developing growth factor carriers from naturally derived biomaterials like polysaccharides and gelatins. These materials have demonstrated biocompatibility (accepted by the US Food and Drug Administration) and have shown a number of physico-

# The first two authors contributed equally to this manuscript.
* Correspondence to Dr Fa-ming CHEN.
E-mail cfmsunhh@fmmu.edu.cn
Received 2008-10-11 Accepted 2009-02-01

chemical properties that make them suitable for different clinical applications in drug delivery systems[6–10]. The development of drug delivery systems that can be rapidly transferred to the clinical setting to help patients has considerable economic and therapeutic potential, and natural material-derived substances could be considered prime candidates for such procedures.

We have reported several microsphere systems fabricated from glycidyl methacrylated dextran (Dex-GMA) and/or gelatin for the controlled release of proteins and have demonstrated their advantages both *in vitro* and *in vivo*[6–10]. Based on our experience with the fabrication of microsphere delivery systems, we used the same raw biomaterials (Dex-GMA and gelatin) to synthesize nanoparticle vehicles using a facile method in the present study. As we discussed in a recently published review, the crosslinking of Dex-GMA and gelatin may produce a system that is enzymatically but not hydrolytically degradable[3]. This would therefore provide drug delivery systems that could selectively deliver their contents only at sites where an appropriate biological enzyme is present. Moreover, nano-sized particles are potentially injectable and can enhance the distribution of therapeutic agents when used in anomalistic periodontal defects, thus contributing a more promising tool than the microparticle systems we have reported previously[6–9]. With further *in vivo* studies, the currently discussed nanoparticles may have the potential to become a powerful tool for delivering active drugs to the periodontium.

Materials and methods

Materials Dextran T-70 (Dex, M_W 69800 with 5% branches) was purchased from Xia-si Biochemical Co (Beijing, China); gelatin Type A 250 Bloom (pH_i=8.5, 1% in water) was supplied by Nitta gelatin (Osaka, Japan). BMP-2 (chemical extraction from the cortical bone) with an isoelectric point (IEP) of 5.0 in the form of an aqueous solution (5%, *w/w*) was obtained from the Academy of Military Medical Science (Beijing, China). The chemical modification of dextran with glycidyl methacrylate (GMA) was achieved via our previously reported method, and three types of Dex-GMA differing in degree of substitution (DS; 4.7, 6.3, and 7.8) were prepared[9]. Acrylic acid (AA) (Sinopharm Chemical Reagent Co Ltd, Shanghai, China) was dried by $MgSO_4$ and then vacuum distilled before use. *N,N′*-Methylene bisacrylamide (MBA) (Fluka) was re-crystallized from methanol. Cerium (IV) ammonium nitrate (CAN) was re-crystallized from dilute nitric acid containing ammonium nitrate, all were obtained from Sinopharm Chemical Reagent Co Ltd (Shanghai, China). All other chemicals were of analytical grade and used as received.

Spray freeze-drying of bone morphogenetic protein (BMP) An aqueous solution of BMP-2 was atomized using a two-fluid nozzle in a stainless steel chamber; the processing conditions were chosen to minimize the particle size after the first suspension step in the encapsulation procedures. The slurry was collected in stainless steel beakers and poured into glass dishes, which were lyophilized after pre-cooling the shelves to -40 °C. Dried BMP powders were stored at -20 °C.

Preparation of Dex-GMA/gelatin nanoparticles (DG-NPs) The preparation scheme was carried out from a one-step synthesis of dextran-based stable nanoparticles assisted by self-assembly reported by Tang *et al* (2006) with minor modification[11]. Briefly, 2 mg Dex-GMA(DS=7.8) and 8 mg gelatin were dissolved in 50 mL deionized water at 25 °C under gentle stirring and nitrogen bubbling. Then the solution of 1.0 mL CAN (0.5 mg/mL) in 1.25 mL 0.1 mol/L nitric acid and 1.0 mg AA were successively added. Twenty minutes later, Cerium (IV) was used as an initiator for the graft copolymerization, MBA was added and the reaction was maintained at 30 °C for 4 h. Thereafter, 1 mol/L NaOH was added to neutralize the reaction system. Finally, the resulting suspension was filtered against deionized water for 3 d using a membrane bag with a 14 000 cut-off molecular weight to remove the un-reacted monomers and the un-grafted poly(acrylic acid) (PAA) agitated on a shaker table (70 r/min) at 4 °C. The supernatant was subsequently discarded, and the pellet was resuspended by 10 mL PBS (pH 7.4). The final aqueous solutions were lyophilized to obtain the solid Dex-GMA/gelatin nanoparticles (DG-NPs).

Immobilization of BMP onto DG-NPs BMP was immobilized onto DG-NPs by swelling the nanoparticles in aqueous BMP solutions using the methods previously described[9], in which a polyionic complexation was formed between BMP (with an IEP of 5.0) and an acidic gelatin (with an IEP of 8.5)[12]. Briefly, DG-NPs (5 mg) were mixed with 1 mL of spray freeze-dried BMP (initial concentrations of 0.1, 0.5, 1.0, 1.5, or 2.0 mg/mL) in phosphate-buffered saline (PBS), pH 7.4, and the mixture was incubated at 4 °C for 1 h under moderate stirring. After the adsorptive loading, the BMP-immobilized nanoparticles were washed twice with PBS and resuspended at 10 mg/mL in PBS. Then the amount of loaded BMP was evaluated by the Lowry method[13]. BMP-immobilized nanoparticles were added to the same volume of 4% sodium dodecyl sulfate (SDS) to dissolve the nanoparticles, and the BMP loading content was then determined. The immobilization efficiency (IE) of BMP onto the nanoparticles was calculated as:

$$IE=\frac{\text{BMP amount loaded onto the nanoparticles}}{\text{Initial feeding amount of BMP}}\times 100\%$$

Preparation of BMP-encapsulated DG-NPs To prepare BMP-encapsulated DG-NPs, BMP was added to the reaction system prior to MBA addition, with 2 mL of spray freeze-dried BMP (initial concentrations of 0.1, 0.5, 1.0, 1.5, or 2.0 mg/mL) used for each batch. The BMP loading content was also measured by the aforementioned Lowry method, in which the encapsulated efficiency (EE) of BMP into the nanoparticles was calculated as:

$$EE=\frac{\text{BMP amount encapsulated into the nanoparticles}}{\text{Initial feeding amount of BMP}}\times 100\%$$

Transmission electron microscopy, scanning electron microscopy, and atomic force microscope measurements Unloaded nanoparticles were observed using transmission electron microscopy (TEM) after freeze fracture. A small drop of an aqueous nanoparticle suspension was deposited into a 100-μm-deep symmetric cup. Then the sample was frozen using a high-pressure cooling device HPM 010 (Bal-Tec). Fracturing, etching, and shadowing using platinum carbon (Pt–C) as an activator were performed in a Bal-Tec apparatus (Model BAF 400T). The replicas of the surface were then floated off by ordinally submerging the specimen in successive baths of water/acetone, water, NaOH (1 mol/L), water, and acetone. Finally, the replicas were collected onto naked 400 mesh grids, which were subsequently mounted in a TEM (PHILIPS CM120 BioTwin) for inspection. TEM observations were performed on a LEO 912 Omega high-resolution microscope working at 120 kV. At the same time, dried microspheres were sprinkled onto a piece of electric-glue paper, gold-sprinkled in a vacuum, and examined by scanning electron microscopy (SEM; S-2700, Hitachi, Tokyo, Japan). The freeze-dried particles were mounted on an aluminum sample mount and sputter-coated with gold-palladium to minimize surface charging. The morphologies and size of the DG-NPs and BMP-immobilized nanoparticles were also observed by atomic force microscope (AFM; Aijian Nanometer Co, Shanghai, China), in which a drop of the nanoparticle suspension was placed on a copper grid coated with collodion and was negatively stained by 1% ammonium molybdate.

Particle size analysis A freshly prepared suspension of DG-NPs was analyzed for particle size and size distribution by the light scattering method (90Plus particle size analyzer; Brookhaven Corp, Holtsville, NY). The nanoparticle suspension was diluted 10- to 20-fold with an ethanol-water mixture (65:35 *v*/*v*), and particle size analysis was conducted using a scattering angle of 90° and temperature of 25 °C.

Zeta-potential of DG-NPs The zeta potential of the resultant nanoparticles was measured by a Malvern Zetasizer 2000. The nanoparticles were dissolved in buffers with different pH values to keep the pH constant during measurement. Each sample was measured five times, and the values reported are the average values of these measurements.

Nanoparticle degradation Three batches of DG-NPs were incubated in PBS (pH 7.4) or PBS containing approximately 0.1 U/mL dextranase (pre-equilibrated to 37 °C) and then incubated under continuous shaking in an oscillating water bath (GFL 1092; 100 r/min) at 37 °C[9]. At d 1, 2, 3, 5, 7, 10, and 12, specimens (n=3 for each batch) were removed from the buffers for measurement. The wet weight (Ww) immediately upon removal from the buffer and dry weight (Wd) after 24 h of vacuum-drying were recorded for each specimen. Accordingly, the fold swelling ratio of DG-NPs at each time point was calculated by the following equation: swelling ratio (Rs)=$(Ww–Wd)/Wd$. This value provides a means of assessing the ratio of water (g) per gram of dry DG-NPs in each batch at the corresponding time point. Additionally, the percent of DG-NP mass loss at each time point was determined from the following equation: % DG-NP mass loss=$(Wx–Wd)/Wx$, where Wx is the initial weight of DG-NP (before placement in the buffer).

***In vitro* release study of BMP-immobilized nanoparticles** The release experiment was carried out following the method reported in our earlier publication[9] and performed *in vitro* as follows. BMP-immobilized nanoparticles (10 mg) were suspended in 1 mL of PBS in the absence or presence of dextranase (0.1 U/mL, Sigma Chemicals) and placed in a microtube. The concentration of BMP was 1.2 mg/mL of nanoparticle suspension. The tubes were incubated at 37 °C under moderate stirring. At different time intervals, 100 μL samples were withdrawn and centrifuged at 14 000 r/min for 15 min. The amount of BMP released into the supernatant was determined by the Lowry method. Values were reported as average ±standard deviation.

Cytotoxicity assay with MTT Human periodontal ligament cells (PDLCs) were obtained from premolars extracted for orthodontic reasons from three 14-year-old patients using explant cultures as previously described. The PDLCs used in this study were between the third and fifth passage. The protocol for the studies was approved by the Ethical Committee of Fourth Military Medical University (Xi'an, China). In brief, PDLCs were seeded in 96-well plates at a density of 2×10^4 cells/mL and cultured (37 °C, 5% CO_2) in medium containing 10% fetal bovine serum (FBS). The cells were incubated for 4 h with different concentrations of nanoparti-

cles (0.5–5 mg/mL), then washed three times with PBS and further cultured in medium for 24 h. An aliquot (25 μL) of MTT (3-(4,5-dimethylthiazol-2-yl)-2,5-diphenyltetrazolium bromide) reagent (2.5 mg/mL) was added to the culture medium, and cells were incubated for 2 h. Then the supernatant was removed and the blue formazan product was washed out after 12-h cell lysis with 200 mL SDS (25% in 0.1 mol/L NaOH). The absorbance was measured in a microplate reader at 540 nm. The extinction of the blue dye correlated with the cell viability. Untreated cells served as a reference and were assumed to represent 100% viability, whereas cells treated with paraformaldehyde solution (5%, 15 min) were set to 0% viability. Cells treated with the lysis reagent alone served as controls. The data were expressed as cell viability relative to the reference cells.

Results

Characteristics of DG-NPs The morphology of freeze-dried DG-NPs was characterized using TEM, SEM, and AFM. Phosphotungstic acid was used as a negatively stained reagent to facilitate TEM observation, and a negatively stained TEM image of DG-NPs is shown in Figure 1. The nanoparticles were well proportioned in size and spherical in shape. When measured by SEM methods, DG-NPs were separated from the suspension by centrifugation and lyophilized. The sputter-coated samples were then observed for surface morphology under SEM. Both samples of nanoparticles demonstrate a spherical morphology with a smooth and uniform surface (Figure 2A). Figure 2B shows the AFM photograph of freeze-dried DG-NPs with a three-dimensionally spherical appearance and a particle diameter less than 100 nm. DG-NPs were also characterized for exact particle size by a Brookhaven 90-Plus particle size analyzer. The mean particle size was 53.7 nm; roughly 60% of the nanoparticles were in a narrower size distribution ranged from 40 to 60 μm (Figure 3).

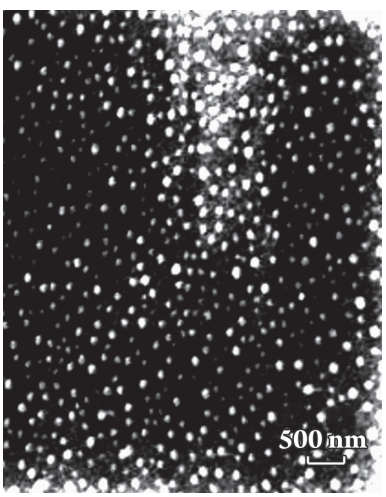

Figure 1. A representative transmission electron microscopic image of unloaded freeze-dried Dex-GMA/gelatin nanoparticles (DG-NPs) following negative staining with 2% (*w*/*v*) phosphotungstic acid (particle diameter less than 100 nm).

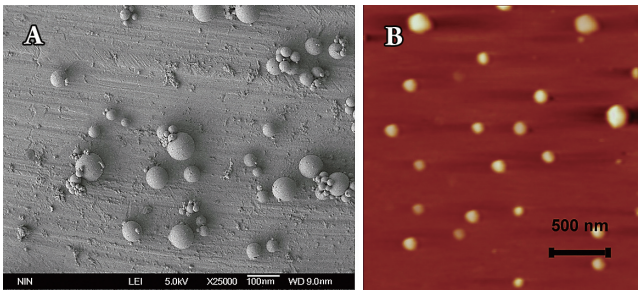

Figure 2. Morphological observations of freeze-dried Dex-GMA/gelatin nanoparticles (DG-NPs) (particle diameters less than 100 nm). (A) A representative scanning electron microscopy image of unloaded DG-NPs. (B) A representative atomic force microscopy image of unloaded DG-NPs.

In our pilot experiments, we found that the degree of substitution (DS) of Dex-GMA has no significant influence on the zeta potential of the resultant DG-NPs. The nanoparticles prepared from Dex-GMA (DS=7.8) and gelatin had strongly negative zeta potentials (-20 mV), which may be attributed to the electrostatic repulsion of basic charged gelatin located near the surface[14].

The IE and EE of BMP showed a significant difference between different entrapment methods (Table 1). These results indicate that encapsulation, in contrast to surface immobilization, appeared to be the main mechanism for

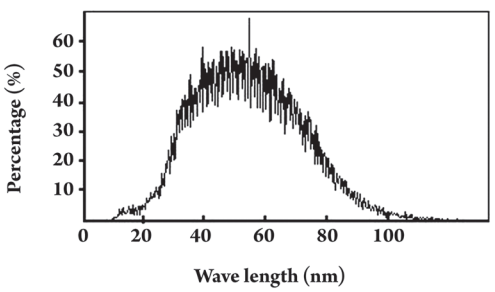

Figure 3. Particle size and size distribution of Dex-GMA/gelatin nanoparticles (DG-NPs) using a Brookhaven-90Plus particle size analyzer (data from a representative batch of DG-NPs). A monodispersed size distribution ranged from 20 to 100 nm in diameter was observed, and more than 60% of the nanoparticles had an even narrower size range of 40 to 60 nm.

Table 1. Final BMP loading (micrograms of BMP per milligram of nanoparticles) to Dex-GMA/gelatin nanoparticles (DG-NPs) achieved by different entrapment methods.

Initial BMP concentration (mg/mL)	0.1	0.5	1.0	1.5	2.0
Immobilization method	19.86±8.72	96.42±24.23	101.68±36.76	107.01± 34.17	103.80±27.72
Encapsulation method	20.63±12.47	102.66±32.79	203.97±24.62[b]	255.37±12.78[c]	248.64±15.55[c]

Significant differences between different protein entrapment method (data are shown as mean±SD): [b]$P<0.05$, [c]$P<0.01$.

loading proteins into the DG-NPs. The maximum amount of BMP immobilization onto the nanoparticle surface was roughly 100 μg of BMP per milligram of DG-NPs at maximum. When the encapsulation method was used, however, these values reached roughly 250 μg of BMP per milligram of DG-NPs (Table 2).

Since the bioactivity of growth factors must be retained during their processing and release from the delivery system, it is essential that the fabrication for processing the carrier does not damage the growth factors. However, encapsulation of growth factors into carriers often leads to a loss of bioactivity[3]. Therefore, the preferred method involves incorporating the growth factor into the vehicle after fabrication. Taking the final required concentration of BMP for periodontal regeneration into consideration, 100 μg of BMP per milligram of DG-NPs is sufficient for our final applications. The immobilization method was therefore applied for BMP loading in the following experiments.

Swelling and DG-NP mass loss Figure 4A and 4B demonstrate the swelling and mass loss profiles of DG-NPs in standard PBS. After the initial 24 h, equilibrium swelling ratios (Rs) were approximately 18-fold and mass loss values between 10% and 15%. Over the following 11 d, the swelling ratios and DG-NP masses remained fairly constant. However, large swelling ratios and mass loss values were observed in PBS containing dextranase (Figure 4C, 4D). The swelling ratio of DG-NPs was (29.9±7.3)-fold at the end of phase 2 (d 2) and quickly reached 42.3-fold after 5 d of incubation. By the end of phase 3 (d 12), these nanoparticles were completely degraded.

Table 2. The BMP loading efficiencies (%) of Dex-GMA/gelatin nanoparticles (DG-NPs) achieved by different entrapment methods.

Initial BMP concentration (mg/mL)	0.1	0.5	1.0	1.5	2.0
Immobilization efficiency (IE)	99.31	96.42	50.84	35.67	25.95
Encapsulation efficiency (EE)	99.85	99.38	98.72[b]	82.44[c]	60.17[c]

Significant differences of BMP loading efficiencies between different protein entrapment methods: [b]$P<0.05$, [c]$P<0.01$.

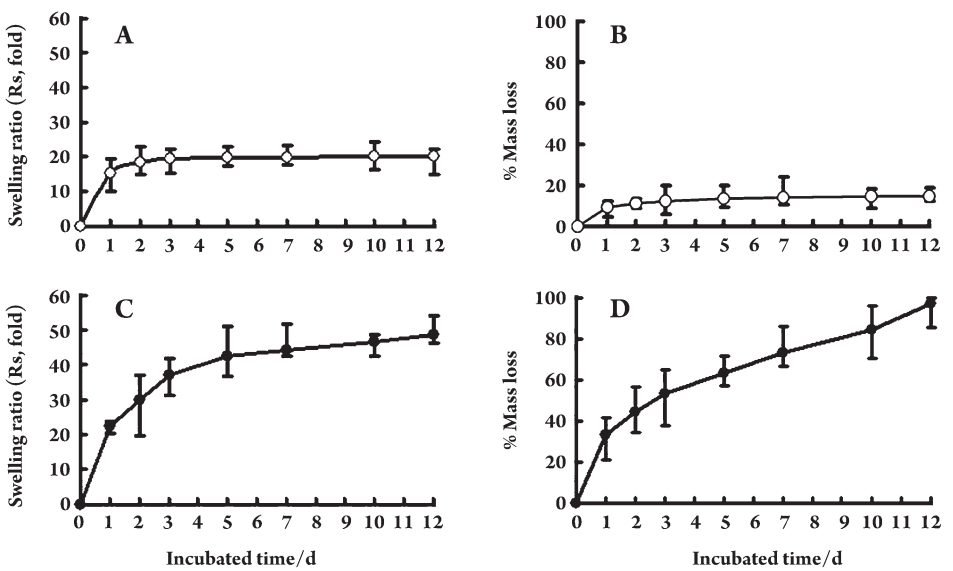

Figure 4. *In vitro* swelling (swelling ratio, Rs) and degradation (% mass loss) profiles of Dex-GMA/gelatin nanoparticles (DG-NPs) in PBS (A and B) or PBS containing dextranase at a concentration of approximately 0.1 U/mL (C and D). Data are from three representative batches, and values are expressed as mean±standard deviation of three batches performed in three independent experiments.

Release behavior of BMP-immobilized DG-NPs To study protein release behavior, BMP-immobilized DG-NPs (96.42 μg of BMP per milligram of DG-NPs) were simply suspended in PBS in the presence or absence of dextranase. BMP release was determined by an *in vitro* dynamics method. The release of BMP from nanoparticles with a BMP content of 100 μg per milligram of DG-NPs was carried out at 37 °C in PBS (pH 7.4). BMP release from BMP-immobilized nanoparticles occurred in a very slow manner, with cumulative release less than 20% during the 12 d (Figure 5). Additionally, the DS of Dex-GMA did not influence this release behavior in PBS in the absence of dextranase (data not shown), and the same phenomenon was found in our previous release studies of insulin-loaded dextran-co-gelatin microspheres[9]. Accordingly, since dextran-co-gelatin biomaterial is enzymatically degraded[9], the final release of BMP from DG-NPs is expected only when the medium contains a hydrolyzing enzyme like dextranase.

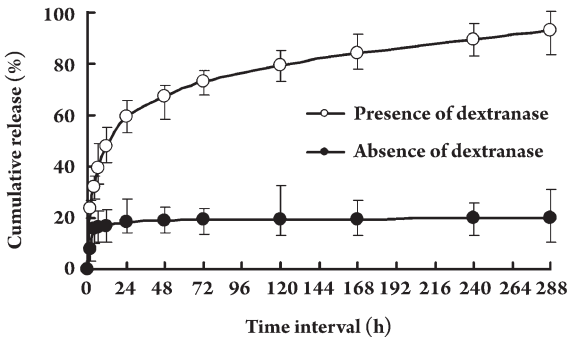

Figure 5. *In vitro* BMP release profiles of BMP-immobilized Dex-GMA/gelatin nanoparticles (DG-NPs) in standard phosphate buffer in the presence or absence of dextranase (pH 7.4) during a time period of 12 d. Individual points represent the mean values±standard deviation from four DG-NP samples.

As shown in Figure 5, DG-NPs exhibited relatively constant BMP release profiles in standard PBS in the presence of dextranase. Burst release values for the DG-NPs were 47.9%±5.7%; thereafter, a slower maintained BMP release (phase 2 and 3 release) was observed over a 12-d release period. Specifically, we found that DG-NPs exhibited a burst release, a phase 2 release rate of approximately 5.0% per day from d 1 to d 3, and a phase 3 release rate of approximately 0.4% per day from d 4 to d 12. In fact, the final cumulative release value for DG-NPs was more than 90%. For longer release times, we found the final cumulative release to be approximately 100% (after 20 d; data not shown). This finding indicates that DG-NPs can be completely biodegraded in 20 d in the presence of dextranase. However, the BMP release profiles in standard PBS in the absence of dextranase showed kinetics with only a significant burst and very slow release after the initial burst release (Figure 5); these kinetics suggest that the BMP release from DG-NPs may be controlled by biodegradation properties.

***In vitro* cytotoxicity test** The biocompatibility of the nanoparticles was evaluated *in vitro* by a cytotoxicity test using PDLCs. The surviving cells after incubation were evaluated by an MTT assay. PDLC proliferation and viability as a function of the concentration of 0.5, 1, and 5 mg/mL empty and BMP-immobilized nanoparticles after 24 h of incubation were investigated. Cell proliferation was not affected by either nanoparticle, and cellular viability was maintained at levels higher than 85%. However, a significant dose-dependent effect on cell viability was observed for BMP-immobilized nanoparticle preparations ($P<0.01$) (Figure 6). This finding implies that these nanoparticles can be useful as protein carriers without any significant cytotoxic effects and can protect the bioactivity of loaded proteins.

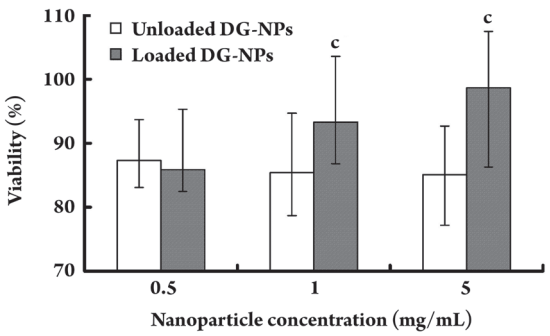

Figure 6. Cytotoxicity of BMP-immobilized Dex-GMA/gelatin nanoparticles (DG-NPs) (unloaded and BMP-loaded) as evaluated *in vitro* by a cytotoxicity test using periodontal ligament cells (PDLCs). The cell viability results are shown after PDLC incubation with three different concentrations ranging from 0.5 to 5.0 mg/mL for a period of 24 h. Data are shown as mean values±standard deviation ($n=8$). $^{c}P<0.01$, compared with unloaded nanoparticle preparations.

Discussion

Significant effort has been devoted in recent years to develop nanotechnologies for drug delivery because they offers a suitable means of delivering small molecular weight drugs as well as macromolecules like proteins, peptides, or genes by either localized or targeted delivery to tissues of interest[4, 5, 15]. In general, nanoparticles can be used to provide localized delivery of biomolecules to targeted tissues, to solubilize drugs for intravascular delivery, and to improve the stability of therapeutic agents, especially proteins, peptides, and nucleic acid drugs, against enzymatic degradation

(nucleases and proteases)[4]. The nanometer size ranges of these delivery systems offer certain distinct advantages for drug delivery in tissue engineering and regenerative medicine. Due to their sub-cellular and sub-micrometer size, nanoparticles demonstrate relatively greater intracellular uptake than microparticles and are generally taken up efficiently by the cells[15]. This permits efficient delivery of therapeutic agents to target sites in the body[16]. Additionally, by modulating polymer characteristics one can control the release of a therapeutic agent from nanoparticles to achieve desired therapeutic levels in target tissue for a duration sufficient for optimal therapeutic efficiency[4, 5]. Further, nanoparticles can be delivered to distant target sites either by localized delivery using a catheter-based approach with a minimally invasive procedure or by conjugation to a biospecific ligand that can direct them to the target tissue or organ[4, 16]. Therefore, nanoparticles may have more widespread applications in the drug delivery, regenerative medicine, and tissue engineering fields. For these reasons we are interesting in developing a new BMP nano-carrier in spite of the good results we have already obtained from our dextran-co-gelatin microspheres[6,9].

Using a facile self-assembly-assisted approach, Dex-GMA/gelatin nanoparticles were successfully synthesized in the present study directly from monomers without the use of any organic solvents or surfactants. The resultant nanoparticles had a strongly negative zeta potential (-20 mV), which can be attributed to the electrostatic repulsion of basic charged gelatin located near the surface. The structure of the nanoparticles may consist of a dextran-based core with an outer gelatin shell. The zeta potential value is an important particle characteristic because it can influence particle stability. Electrostatic repulsion between particles with the same electric charge prevents the aggregation of these particles[14]. To investigate the distribution of gelatin on the surface, the nanoparticles were suspended in buffers of varying pH values (pH 4–8) and the zeta potential was then determined. The zeta potential did not change at pH values ranging from 5 to 8. However, it increased with a decrease in pH from 4 to 5 and reached -7 mV at a pH of 4. The change in the zeta potential might be due to the ionization of gelatin located near the surface, but such a core-shell configuration requires more convincing evidence. During the swelling and degradation tests, we observed a phenomenon very similar to that was found in the dextran-co-gelatin microspheres investigated in our previous studies[7, 9]. DG-NPs are only degraded in PBS in the presence of dextranase, and good agreement between the experimentally measured and theoretically presumed protein release kinetics was obtained.

The entrapment of BMP onto the nanoparticles was successfully achieved in our study. In comparison to unloaded nanoparticles, the BMP-loaded nanoparticles did not change significantly with regard to particle size and showed a monomial size distribution. Our results demonstrated that the entrapment efficiency of BMP was significantly dependent on the conjugation method (*ie*, immobilization or encapsulation). It can be surmised that the IE was mainly determined from the surface area of the DG-NPs. In the case of BMP surface immobilization, the theoretical amount of BMP immobilized onto the surface may increase as particle size decreases. In fact, the IE we observed had a maximum of roughly 100 μg of BMP per milligram of DG-NP. When we used the encapsulated method, the amount of BMP encapsulated into the nanoparticles was roughly 250 μg per milligram of DG-NPs at maximum(initial BMP concentration 2 mg/mL). The loading capacity of BMP into the nanoparticles was significantly higher than the maximum amount of BMP immobilized onto the surface (P<0.01). Therefore, we conclude that the inner space of the nanoparticles had great potential to load the proteins. This result indicates that encapsulation, in contrast to surface immobilization, appeared to be the main mechanism for loading protein. Surface immobilization should be the first choice when the bioactivity of the loaded proteins is taken into consideration, however, provided that 1) drug loading can meet the requirements of the final applications and 2) the immobilized mechanism can provide sustained drug release for the required period.

The interaction between BMP and the nanoparticles is very stable, possibly due to electrostatic interactions between the acidic BMP and the basic gelatin groups[12]. The gelatin used in this study had an IEP of 8.5 and was thus a "basic" gelatin. As a result, BMP (with an IEP of about 5.0) can be well absorbed to the basic gelatin hydrogel with time during both entrapment processes. This can be explained in terms of the electrostatic interaction between the positively charged growth factors and the gelatin[9, 12]. For this reason, our final BMP immobilization levels reached roughly 100 μg of BMP per milligram of DG-NPs. Dextran is a natural polysaccharide, and the characteristic α-1,6-glucosidic linkage is hydrolyzed by dextranase[11]. Experiments have indicated that derivative dextrans can also be degraded by dextranase and that an increasing degree of substitution results in a slower degradation rate[11]. We hope to use the advantages of both gelatin (*ie*, ionic interaction between oppositely charged molecules) and dextran (*ie*, enzyme degradation without rapid solubilization) to generate an enhanced composite biomaterial that can release drug molecules in the colon after

hydrolysis of the polysaccharide nanoparticles by dextranase.

As anticipated, less than 20% of the incorporated BMP was desorbed from DG-NPs within the initial 24 h under *in vitro* non-degradation conditions (PBS in the absence of dextranase). This was followed by a lack of further substantial desorption, whereas a large initial desorption of incorporated drugs was observed for simplex dextran-derived microspheres[8]. We thus conclude that the BMP immobilized to the basic gelatin hydrogel through ionic interaction was released *in vivo* mainly as a result of micro-carrier degradation. Therefore, the absence or slow release of BMP from the nanoparticles in PBS can be understood as a consequence of the interaction between the protein and the Dex-GMA/gelatin grafts. In fact, several studies have shown that the Dex-GMA/gelatin hydrogel is not degraded in a neutral buffer[7, 9]. In our previous study we also observed that dextran-based microparticles are degraded by dextranase, an enzyme widely distributed among living organisms that catalyzes the hydrolysis of γ-glutamyl compounds[8]. It is expected that protein-encapsulated DG-NPs can release protein in the cell or *in vivo* by the introduction of enzymes like dextranase. As shown in Figure 4, DG-NPs are presumably only degraded in PBS containing dextranase. These results indicate that the release of proteins from DG-NPs is controlled primarily enzymatically during the entire release period and that different speeds of enzymatic degradation result in different release rates.

It has been reported that spontaneous regeneration of 50% to 70% can be expected in an acute defect model, and local application of growth factors like BMP can promote periodontal tissue regeneration[1-3]. The mechanisms driving this regeneration are unclear. The development of ossification in periodontal defects is itself a complex biological process that requires intricately regulated interactions between cells, locally acting growth factors, mechanical loading (*eg*, pressure and tension forces), systemic hormones and growth factors, and the matrix components in which these entities interact[13, 14]. However, it is certain that BMP in DG-NPs may spread evenly from the periodontal defect and, over time, stimulate new bone formation in tissue where pooling or localized accumulation of BMP did not occur. Therefore, the loaded BMP may be utilized by the surrounding cells or tissues more efficiently. To evaluate the biological effects of BMP in DG-NPs on periodontal wound healing *in vivo*, animal experiments should be performed before any further preclinical experiments are taken into consideration. Future work should focus on precisely localized growth factor delivery by nanoparticles, and applications of these nanoparticles in both bone and periodontal repair should be emphasized. This is an area, along with the tissue engineering and regenerative fields, in which the clinical usage of growth factors could have great impact in the near future.

For local delivery of bioactive drugs, the carrier must be clinically and mechanically manageable, biologically acceptable, and able to support wound stability[2]. It is promising that our implanted DG-NPs are able to protect loaded biomolecules from degradation and release them for extended time periods. In light of our previous study, dextran-co-gelatin has proven to be a good biomaterial for the controlled release of several biologically active molecules[9, 17]. While work continues to improve its release technology through the use of composite scaffolds and biomaterial modification, more studies are required to characterize the sorption and release profiles of a wider variety of biomolecules from this carrier[18, 19]. The utility and potential of nanoparticle drug delivery systems have been demonstrated, and it has been shown that tailored delivery is possible[20–23]. Many chemical and engineering questions specific to these designed systems have been addressed[24, 25]. The broad scope application of micro/nano-systems requires testing in case-by-case studies, and it may not always be clear how systems will perform during *in vivo* tests compared to controlled, laboratory environments[26–29]. However, synthesizing delivery systems for active drugs and promoting their application for the treatment of different bone defects is a realistic prospect.

Conclusion

Novel dextran- and gelatin-based copolymers formed nanoparticles with a mean diameter of roughly 53.7 nm and a mono-dispersed size distribution when prepared using a facile synthesis method assisted by self-assembly. The DG-NPs showed a highly negative zeta potential in PBS. BMP was successfully entrapped onto these nanoparticles and demonstrated sustained release for 12 d under degradation conditions. *In vitro* cytotoxicity testing showed that the present nanoparticles did not induce any cytotoxicity against PDLCs. Thus, these DG-NPs may be considered promising biodegradable and biocompatible protein carriers for modulated biodistribution as well as site- and/or cell-specific drug delivery systems. With further studies, these nanoparticles may have the potential to serve as candidate growth factor-vehicles for periodontal tissue regeneration enhancement.

Acknowledgements

This project was supported by a grant from the Chinese

National Natural Science Foundation (No 30700173), as well as grants from the contributor's own institution.

Author contribution

Dr Fa-ming CHEN and Prof Zhi-fen WU designed the research; Dr Fa-ming CHEN, Dr Zhi-wei MA, and Prof Guang-ying DONG performed the research; Dr Fa-ming CHEN analyzed the data; Dr Fa-ming CHEN and Dr Zhi-wei MA wrote the paper.

References

1 Tabata Y. Significance of release technology in tissue engineering. Drug Discov Today 2005; 10: 1639–46.
2 Vasita R, Katti DS. Growth factor-delivery systems for tissue engineering: a materials perspective. Expert Rev Med Devices 2006; 3: 29–47.
3 Chen FM, Shelton RM, Jin Y, Chapple IL. Localized delivery of growth factors for periodontal tissue regeneration: role, strategies, and perspectives. Med Res Rev 2009; 29 (in print). doi: 10.1002/med.20144.
4 Mundargi RC, Babu VR, Rangaswamy V, Patel P, Aminabhavi TM. Nano/micro technologies for delivering macromolecular therapeutics using poly(*D*,*L*-lactide-co-glycolide) and its derivatives. J Control Release 2008;125:193–209.
5 Jabr-Milane L, van Vlerken L, Devalapally H, Shenoy D, Komareddy S, Bhavsar M, *et al*. Multi-functional nanocarriers for targeted delivery of drugs and genes. J Control Release 2008; 130: 121–8.
6 Chen FM, Wu ZF, Wang QT, Wu H, Zhang YJ, Nie X, *et al*. Preparation and biological characteristics of recombinant human bone morphogenetic protein-2-loaded dextran-co-gelatin hydrogel microspheres, *in vitro* and *in vivo* studies. Pharmacology 2005; *75: 133–44.*
7 Chen FM, Wu ZF, Wang QT, Wu H, Zhang YJ, Nie X, *et al*. Preparation of recombinant human bone morphogenetic protein-2 loaded dextran-based microspheres and their characteristics. Acta Pharmacol Sin 2005; 26: 1093–103.
8 Chen FM, Wu ZF, Sun HH, Wu H, Xin SN, Wang QT, *et al*. Release of bioactive BMP from dextran-derived microspheres: a novel delivery concept. Int J Pharm 2006; 307: 23–32.
9 Chen FM, Zhao YM, Wu H, Deng ZH, Wang QT, Zhou W, *et al*. Enhancement of periodontal tissue regeneration by locally controlled delivery of insulin-like growth factor-I from dextran-co-gelatin microspheres. J Control Release 2006; 114: 209–22.
10 Huang S, Deng T, Wu H, Chen F, Jin Y. Wound dressings containing bFGF-impregnated microspheres. J Microencapsul 2006; 23: 277–90.
11 Tang MH, Dou HJ, Sun K. One-step synthesis of dextran-based stable nanoparticles assisted by self-assembly. Polymer 2006; 47: 728–34.
12 Young S, Wong M, Tabata Y, Mikos AG. Gelatin as a delivery vehicle for the controlled release of bioactive molecules. J Control Release 2005; 109: 256–74.
13 Basinska T, Slomkowski S. The direct determination of protein concentration for proteins immobilized on polystyrene microspheres. J Biomater Sci Polym Ed 1991; 3: 115–25.
14 Feng SS, Huang G. Effects of emulsifiers on the controlled release of paclitaxel (Taxol) from nanospheres of biodegradable polymers. J Control Release 2001; 71: 53–69.
15 Panyam J, Labhasetwar V. Biodegradable nanoparticles for drug and gene delivery to cells and tissue. Adv Drug Deliv Rev 2003; 55: 329–47.
16 Biondi M, Ungaro F, Quaglia F, Netti PA. Controlled drug delivery in tissue engineering. Adv Drug Deliv Rev 2008; 60: 229–42.
17 Wu H, Zhang Z, Wu D, Zhao H, Yu K, Hou Z. Preparation and drug release characteristics of pingyangmycin-loaded dextran cross-linked gelatin microspheres for embolization therapy. J Biomed Mater Res B Appl Biomater 2006; 78: 56–62.
18 Chen FM, Zhao YM, Sun HH, Jin T, Wang QT, Zhou W, *et al*. Novel glycidyl methacrylated dextran (Dex-GMA)/gelatin hydrogel scaffolds containing microspheres loaded with bone morphogenetic proteins: formulation and characteristics. J Control Release 2007; 118: 65–77.
19 Chen FM, Zhao YM, Zhang R, Jin T, Sun HH, Wu ZF, *et al*. Periodontal regeneration using novel glycidyl methacrylated dextran (Dex-GMA)/gelatin scaffolds containing microspheres loaded with bone morphogenetic proteins. J Control Release 2007; 121: 81–90.
20 Huang M, Wu W, Qian J, Wan DJ, Wei XL, Zhu JH. Body distribution and *in situ* evading of phagocytic uptake by macrophages of long-circulating poly (ethylene glycol) cyanoacrylate-co-n-hexadecyl cyanoacrylate nanoparticles. Acta Pharmacol Sin 2005; 26: 1512–8.
21 Jiang B, Hu L, Gao C, Shen J. Crosslinked polysaccharide nanocapsules: preparation and drug release properties. Acta Biomater 2006; 2: 9–18.
22 Huang ZR, Hua SC, Yang YL, Fang JY. Development and evaluation of lipid nanoparticles for camptothecin delivery: a comparison of solid lipid nanoparticles, nanostructured lipid carriers, and lipid emulsion. Acta Pharmacol Sin 2008; 29: 1094–102.
23 Satarkar NS, Zach Hilt J. Hydrogel nanocomposites as remote-controlled biomaterials. Acta Biomater 2008; 4: 11–6.
24 Zhang J, Misra RD. Magnetic drug-targeting carrier encapsulated with thermosensitive smart polymer: core-shell nanoparticle carrier and drug release response. Acta Biomater 2007; 3: 838–50.
25 Zhang J, Rana S, Srivastava RS, Misra RD. On the chemical synthesis and drug delivery response of folate receptor-activated, polyethylene glycol-functionalized magnetite nanoparticles. Acta Biomater 2008; 4: 40–8.
26 Li SH, Cai SX, Liu B, Ma KW, Wang ZP, Li XK. *In vitro* characteristics of poly(lactic-co-glycolic acid) microspheres incorporating gelatin particles loading basic fibroblast growth factor. Acta Pharmacol Sin 2006; 27: 754–9.
27 Juillerat-Jeanneret L, Schmitt F. Chemical modification of therapeutic drugs or drug vector systems to achieve targeted therapy: looking for the grail. Med Res Rev 2007; 27: 574–90.
28 Cui LJ, Sun NX, Li XH, Huang J, Yang JG. Subconjunctival sustained release 5-fluorouracil for glaucoma filtration surgery. Acta Pharmacol Sin 2008; 29: 1021–8.
29 Bailey MM, Berkland CJ. Nanoparticle formulations in pulmonary drug delivery. Med Res Rev 2009; 29: 196–212.